ELSEVIER

Journal of Hydrology 184 (1996) 189–208

Journal of Hydrology

Wetland evaporation and energy partitioning: Indiana Dunes National Lakeshore

Catherine Souch[a,*], Charlotte P. Wolfe[b], C. Susan B. Grimmond[c]

[a]*Department of Geography, Indiana University Purdue University Indianapolis, 213 Cavanaugh Hall, Indianapolis, IN 46202, USA*

[b]*School of Public and Environmental Affairs, Indiana University, Bloomington, IN 47405, USA*

[c]*Climate and Meteorology Program, Department of Geography, Indiana University, Bloomington, IN 47405, USA*

Received 25 February 1995; accepted 29 October 1995

Abstract

For most wetlands precipitation and evapotranspiration are the major components of water gain and loss. However, studies of the hydrology of wetlands largely ignore evaporation, or calculate it by difference or some very simple measure. As part of an integrated study of the hydrology and ecology of wetlands in the Indiana Dunes National Lakeshore, evaporation was measured directly as its energy equivalent, the latent heat flux, using eddy correlation techniques for a 10 day period in June 1994. In addition, data were collected on the other surface energy balance fluxes (net all-wave radiation and sensible heat flux), and ancillary meteorological variables (wind speed and direction, temperature, pressure, relative humidity, solar radiation and water depth). Overall, latent heat flux dissipated 48% of the available radiant energy, storage heat flux 35%, and sensible heat flux 17%. A simple hysteresis model for the storage heat flux was developed which performed extremely well. Proximity to Lake Michigan resulted in evaporation rates close to the equilibrium rate (average Priestley–Taylor α = 1.035), which were affected strongly by net all-wave radiation. Three commonly used models of evaporation, Penman, Priestley–Taylor (α = 1.26) and equilibrium (α = 1.0) are evaluated. The relative success of the equilibrium model, with its limited data requirements, offers great potential for longer-term modeling of water and energy exchanges in this type of wetland environment.

1. Introduction

Wetland hydrology is a primary driving force influencing wetland ecology, its development and persistence. Increased demand for agricultural and domestic water supplies,

* Corresponding author.

PII 0022-1694(95)02989-3

the use of wetland systems in waste water treatment, and speculation about the effects of climate change, have raised awareness of the need for accurate estimates of wetland hydrological fluxes. For most wetlands evapotranspiration is the major component of water loss, and when considered as its energy equivalent, the latent heat flux, the major energy sink (Wessel and Rouse, 1993). Yet despite an extensive number of studies (see reviews by Linacre (1976) and Ingram (1983)), in general, evaporation from wetlands is poorly understood (Lafleur, 1990a), and detailed studies of the physical processes involved remain restricted to a limited range of geographic environments.

In those studies where evaporation is considered explicitly, methods used to measure or model evaporation vary considerably, with significant implications for the accuracy of the results. In many cases, evaporation is not measured directly but is determined as a residual (see, e.g. review by Winter (1981)). The most direct method for obtaining the rate of evaporation uses the eddy correlation approach (WMO, 1966). However, the method requires high-quality instrumentation, and is most applicable to studies of short time periods rather than long-term monitoring. Consequently, the technique has been little used in wetland environments.

As part of an integrated study of the hydrology and ecology of the Great Marsh of the Indiana Dunes National Lakeshore, measurements of the latent heat flux (evapotranspiration) were undertaken using eddy correlation equipment. The overall objective of the study is to examine the relations between wetland hydrology and vegetation, and the role of anthropogenic disturbance in determining wetland plant community composition. The purpose of this paper is to present the results of the first set of micrometeorological measurements, to consider the controls on evaporation in this region, and to assess simple methods to model the flux in such an environment.

2. Methods

2.1. Study area

Indiana Dunes National Lakeshore, located in northern Indiana along 25 km of Lake Michigan's shoreline (Fig. 1), was authorized in 1966 by Congress to preserve remnants of a unique lacustrine ecosystem and provide educational and recreational opportunities near large urban areas. Within this area wetlands occupy interdunal areas, although extensive drainage and ditching before the establishment of the National Lakeshore has drained many wetlands. The most extensive wetland is the Great Marsh (32 km long, an average of 0.8 km wide) (Fig. 1), which is composed of several distinct watersheds which have undergone varying degrees of disturbance.

This study was conducted in the Dunes Creek watershed (Fig. 1). This area, located within Indiana Dunes State Park, has been the least affected by disturbance of all the Great Marsh watersheds. Although ditching has occurred in the past, the area has largely recovered and contains diverse flora (Wilhelm, 1990). The surficial geology of the Great Marsh consists of non-uniform paludal deposits of 0.3–1.5 m depth, on top of unconsolidated glacial, lacustrine and eolian deposits (Thompson, 1987). Existing hydrological information on the Great Marsh indicates it is a discharge zone for both shallow groundwater from

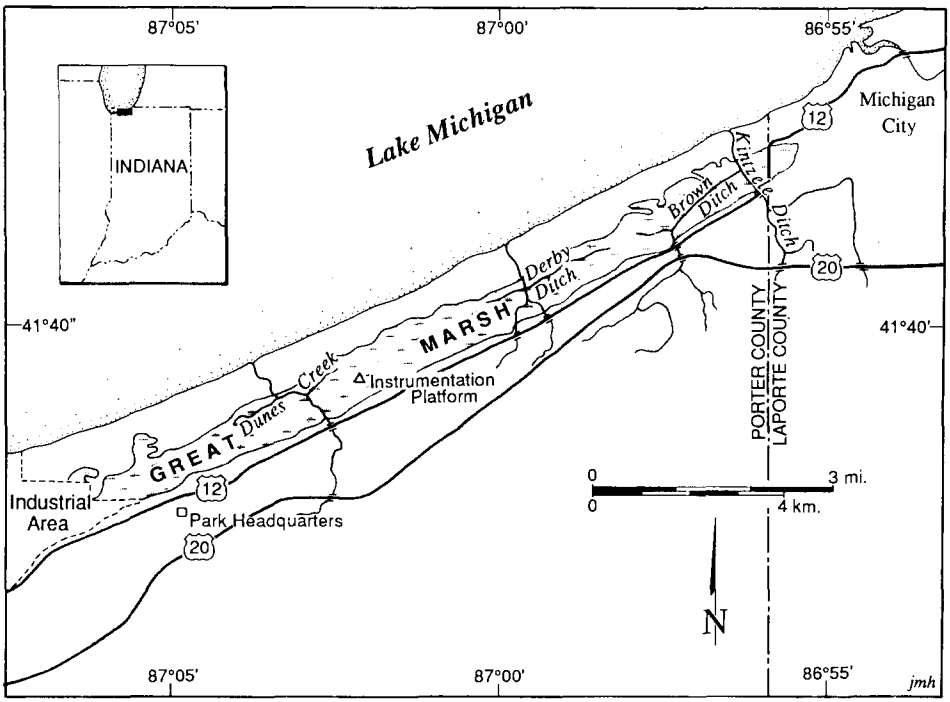

Fig. 1. The Great Marsh and location of the instrumentation platform (adapted from Shedlock et al. (1994)).

adjacent dune complexes, and water from deeper semi-confined aquifers (Loiacono, 1986). Average water depth throughout the undrained portions of the marsh ranges on average from 0.3 to 1.0 m, varying with inflows and outflows, precipitation, and evaporation loss (Shedlock et al., 1994).

The vegetation in the less disturbed portion of the Great Marsh consists of submergent open water, emergent marsh, sedge meadow, scrub–shrub wetlands, and hydromesophytic swamp forest. Open water areas are dominated by submergent aquatic vegetation such as *Potamogeton* spp. (pondweed) and *Ceratophyllum demersum*, floating leaved *Lemna* spp., grading into areas of emergents including *Sagittaria latifolia*, *Nuphar advena*, and *Polygonum* spp. These emergents are similarly found in the emergent marsh areas. Floating mats within the open water areas often provide substrate for these emergents as well as for *Typha* spp., *Carex* spp., and aquatic shrubs such as *Decodon verticillatus* (swamp loosestrife) and *Cephalanthus occidentalis* (buttonbush). As the floating mats recede and the water becomes shallower, the areas are classified as scrub–shrub wetlands. In addition to the same shrubs mentioned as occurring on the floating mats, *Rosa palustris* (swamp rose) is common in the scrub–shrub wetland areas. In the vicinity of the measurement site, the vegetation forms islands several meters across, and covers approximately 50% of the surface area of the Marsh. During the observation period, the average height of the vegetation was approximately 1 m, with the tallest vegetation extending 1.5 m above the water surface (Fig. 2).

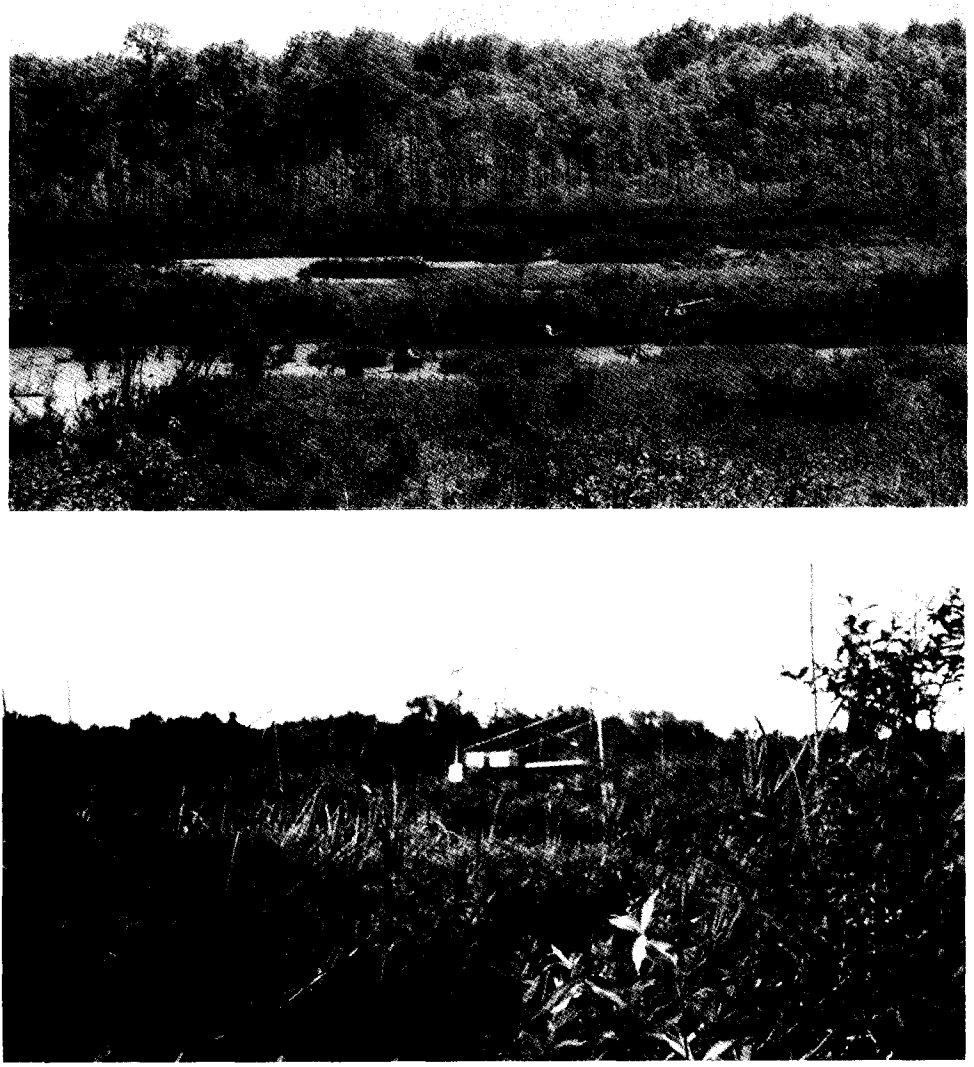

Fig. 2. Upper photo: view looking south across the Marsh from the north bank towards the instrument platform. Lower photo: instrument platform with equipment mounted.

2.2. Instrumentation

In this study, evapotranspiration, referred to hereafter as evaporation, was measured as its energy equivalent, the latent heat flux. Measurements were conducted within the framework of the surface energy balance, which for an extensive homogeneous surface in the absence of advection can be defined as

$$Q^{\downarrow} = Q_H + Q_E + \Delta Q_S \quad [W\ m^{-2}] \tag{1}$$

Table 1
Instrumentation used

Variable	Symbol	Instrumentation
Solar radiation	$K\downarrow$	LI-200S
Net all-wave radiation	Q^*	REBS Q^*6
Sensible heat flux	Q_H	CSI sonic anemometer CA27
Latent heat flux	Q_E	CSI krypton hygrometer KH20
Wind speed and direction	U, Dir	RM Young Wind Sentry
Relative humidity	RH	CSI XN217
Temperature	T	CSI XN217
Water depth	z	PCDR950 pressure transducer
Pressure	P	SBP270 barometric pressure transducer

where Q^* is the net all-wave radiation, Q_H is the sensible heat flux, Q_E is the latent heat flux, and ΔQ_S is the net storage heat flux (which accounts for net storage of energy in the wetland system, in addition to the more usually cited soil heat flux, Q_G). Q_E is related to the mass (water) term E (m s^{-1}) by

$$E = (Q_E)/(L_v \rho) \quad (2)$$

where L_v is the latent heat of vaporization (J kg^{-1}), and ρ the density of water (kg m^{-3}).

In this study, energy balance observations consisted of direct measurements of sensible and latent beat flux, and net all-wave radiation. All equipment was installed at a height of approximately 2 m on a platform located in the center of the marsh, approximately 250 m from the closest edge of the wetland (to the south) (Fig. 1 and Fig. 2; Table 1). The dune ridges which constrain the wetland are vegetated with trees (Fig. 2). The measurement height of 2 m was selected so that the source area for the measurements remained within the wetland, while maximizing the height of the instruments above the vegetation elements.

The convective fluxes (Q_H and Q_E) were measured using eddy correlation techniques (Oke, 1987). A Campbell Scientific Inc. (CSI; Logan, UT) one-dimensional sonic anemometer and fine-wire thermocouple system (SAT: CA27) was used to measure vertical wind velocity and temperature; a CSI krypton hygrometer (KH20) was used to measure the absolute humidity. Fluctuations in the vertical wind velocity, air temperature and humidity were sampled at 5 Hz, and the covariances determined over 15 min periods. Following the procedure of Tanner and Greene (1989), flux corrections were made for oxygen absorption by the sensor, and corrections for air density were made using the method of Webb et al. (1980). Net all-wave radiation was measured with a REBS Q^*6 net radiometer, and incoming solar radiation with a Li-Cor (Lincoln, NE) LI-200S pyranometer. A full error analysis has not been conducted on the Campbell Scientific krypton hygrometer and sonic anemometer, but sources of errors and consideration of their likely magnitudes have been discussed by Roth and Oke (1994). Typical measurement errors for net pyrradiometers are 3–4% (Latimer, 1972).

The standard method of measurement of soil heat flux (Q_G) uses a plate (or plates) buried close to the surface. Halliwell and Rouse (1987) suggested that such an approach seriously underestimates soil heat flux in wetland environments (their study was

Table 2
Average daily and daytime fluxes (MJ m^{-2} day^{-1}), and flux ratios for the measurement period

	Q^*	Q_H	Q_E	ΔQ_s	$Q_H/Q_E\beta$	$Q_H/Q^*\chi$	$Q_E/Q^*\Upsilon$	$\Delta Q_s/Q^*\Lambda$
Daily (24 h)	16.79	2.81	8.14	5.83	0.35	0.17	0.48	0.35
Daytime ($Q^* > 0$)[a]	18.11	2.80	7.33	7.98	0.38	0.15	0.41	0.44

[a] Daylength 14 hours

conducted in permafrost terrain), and sensible and latent heat changes within the soil profile must be accounted for. In this study, given the sub-scale heterogeneity in surface cover (open water of varying depth, vegetation, bare sediment, etc.), it is extremely difficult to measure ΔQ_S directly using such an approach. Here, ΔQ_S is reported as the residual of the energy balance:

$$\Delta Q_S = Q^* - Q_H - Q_E \tag{3}$$

This has the inherent problem that all measurement errors of the other energy balance fluxes are cumulated in the ΔQ_S term, including possible advective effects. Thus the ΔQ_S reported here should be interpreted accordingly.

In addition to the energy balance data, ancillary climate information (wind speed and direction, temperature, pressure, relative humidity, solar radiation, and water depth at the instrument tower) were collected (see Table 1 for information on instrumentation) for the period June 1994–October 1995 for modeling purposes.

2.3. Description of meteorological conditions during study period

Compared with normal, June 1994 was warmer (average temperature 21.9°C, 1.3°C above normal) and wetter (129.5 mm, 25.1 mm greater than normal) (NOAA, 1994, South Bend Local Climatological Data). On 13 June 1994, the day before the measurements started (Year/Day 94/164), a cold front passed through the region. Associated with this, severe thunderstorms resulted in 18.3 mm of rain locally (measured at the Park headquarters; location shown in Fig. 1). Throughout the actual measurement period, the regional-scale flow was dominated by an anticyclone centered over Kentucky, which resulted in hot and humid conditions, with winds predominantly from the southwest. Convective thunderstorms developed in the vicinity of the study area in the afternoon, generally displaced away from Lake Michigan. On the evening of 19 June (94/170) a warm front passed across the region. No rain occurred at the study site. The following day the high pressure rebuilt to the south, and conditions reverted to the hot and humid weather of the previous week. Cloud cover varied both throughout the course of the day, and from day to day (see further discussion below). At the local scale, the diurnal wind pattern is controlled by the presence of Lake Michigan directly to the north of the site. This results in the development of a daytime lake breeze and a nocturnal land breeze.

3. Energy balance fluxes

The observed energy balance fluxes are shown in Fig. 3. The resulting daily (24 h) and

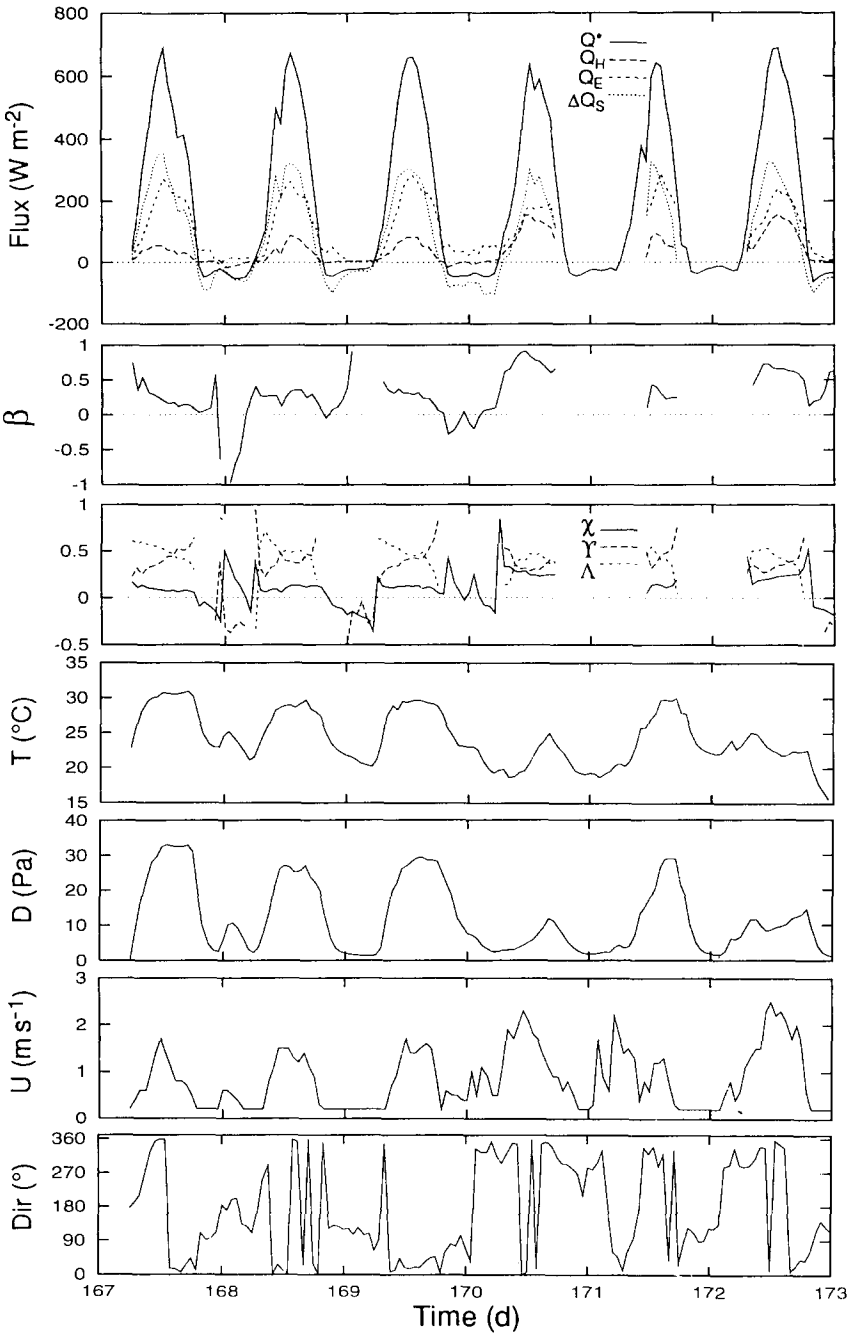

Fig. 3. Time series of energy balance data, flux ratios (β, χ, Λ, Υ), temperature (T), vapor pressure deficit (D), wind speed (U), and wind direction (Dir) for the measurement period.

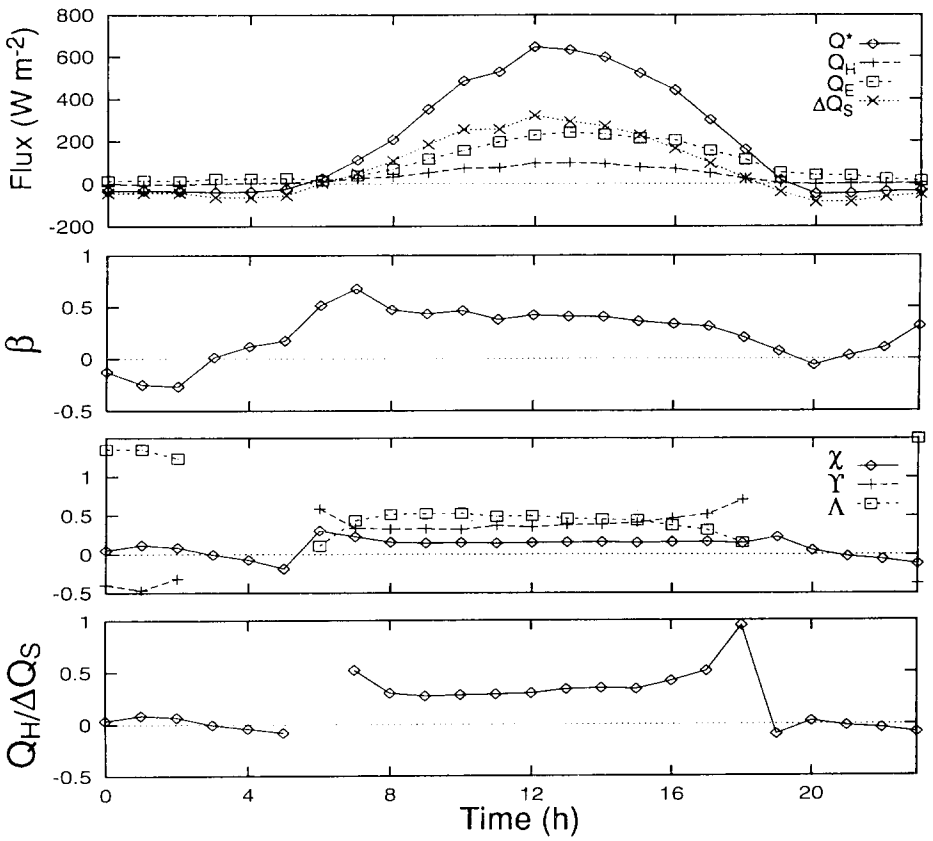

Fig. 4. Ensemble energy balance and flux ratios.

daytime ($Q^* > 0$) fluxes and ratios are summarized in Table 2. Mean (ensemble) flux values and ratios are presented in Fig. 4.

Overall 48% of the net available radiant energy was used in evaporation, 35% in storage, and 17% in the sensible heat flux (Table 2). Observations from individual days are similar in terms of trend and magnitudes, but they are marked by more variability (Fig. 3). Net all-wave radiation is fairly consistent from day to day, although the effects of cloud in the afternoon of 94/170 and morning of 94/171 are apparent. Overall the storage term tends to be the major flux in the morning (Fig. 3 and Fig. 4), peaking at solar noon. It declines through the afternoon and becomes a source of heat 1–2 h before Q^* reverses sign. Evaporation peaks in the early afternoon, with high values through to the early evening. Evaporation remains positive throughout the night, sustained by the large energy release from storage. The sensible heat flux is by far the smallest flux (Fig. 4), and for most of the period is very consistent from day to day (Fig. 3).

The nature of the asymmetry in each of the fluxes is shown clearly in the ratios χ (Q_H/Q^*), Υ (Q_E/Q^*), and Λ ($\Delta Q_S/Q^*$). Similar to previous observations, Λ decreases over the course of the day, whereas Υ increases, and χ remains remarkably constant. For the study

period the average Bowen ratio (β) was 0.35. The diurnal trend of β is fairly constant, with a very slight decrease through the course of the day (Fig. 4).

The hourly latent heat flux is strongly related to net all-wave radiation, and exhibits a positive relationship with temperature, vapor pressure deficit and wind speed (Fig. 5(a)). When plotted against wind direction, evaporation is greater with flows from the north and reduced with winds from the south. However, when Q_E is considered as a fraction of radiant energy, Υ (Q_E/Q^*) (Fig. 5(b)), the variation with wind direction is removed; flows tend to be from the north during the day and associated with the higher daytime evaporation rates, and from the south at night, i.e. lower evaporation rates.

The storage term constitutes 35% of daytime ($Q^* > 0$) fluxes, and 44% of daily (24 h) fluxes. Although in this study the flux was not measured directly, significant warming of the upper water column was noted by researchers as they waded out to the platform to check the equipment. A major problem in comparing the storage term calculated here with values documented in previous studies of wetlands is that the surface characteristics of 'wetlands' vary greatly, most notably in terms of vegetation and the supply of water. In few wetlands is surface water always freely available. The majority of previous micrometeorological studies of wetlands have been conducted in high latitudes with only periodic inundation. Rouse et al. (1987), from studies in southern James Bay and central Hudson Bay, determined the ground heat flux, Q_G, to average 12 and 14% of Q^* over the growing season period; Halliwell and Rouse (1987) documented Q_G at 16–18% of Q^*. In studies of wetlands with standing water always present, Linacre et al. (1970), using data based on one clear day with measurements of the storage term from a lake temperature survey from another, calculated storage at 61% of net radiation, and Silis et al. (1989), in a nearshore intertidal zone of the Western Hudson Bay, estimated heat storage under all conditions to constitute 60% of net radiation.

The partitioning of the sensible to storage heat fluxes (Q_H:ΔQ_S) varies through the course of the day (Fig. 4). In the morning, when the atmosphere is fairly stable and wind speeds are low, the air above the Great Marsh is virtually saturated (Fig. 3). Thus the radiant energy is used to warm the Marsh. Later in the day, as the atmosphere becomes more unstable and the wind picks up, the turbulent transfer of heat into the atmosphere is enhanced and the sensible heat flux becomes more significant.

Differences are evident in the convective flux partitioning between Days 167, 168, 169, and 171, and Days 170 and 172 (Fig. 3(a) and Fig. 3(b)). On Days 170 and 171 temperatures were lower, and the predominant wind direction remained from the north all day. Slightly greater wind speeds but reduced vapor pressure deficits depressed Q_E, with a concomitant increase in the sensible heat flux.

4. Modeling

In many studies of wetland hydrology, evaporation is not measured but modeled using data collected at or near the site. Two simple models that have been used extensively for environments where water is not a limiting factor are those of Penman (1948) and Priestley and Taylor (1972). Both approaches calculate the latent heat flux as a function of

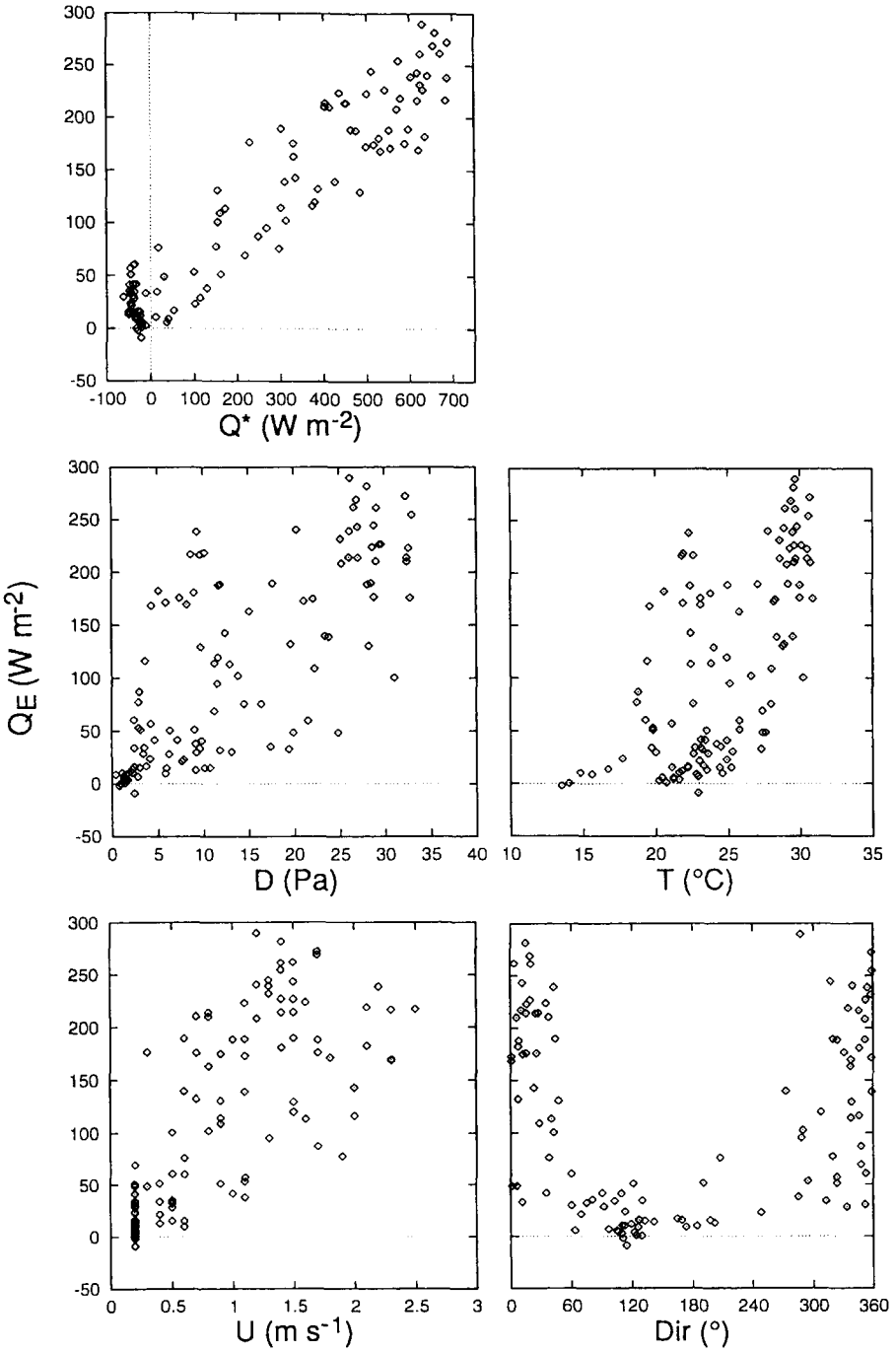
Q* (W m-2)
QE (W m-2)
D (Pa)
T (°C)
U (m s-1)
Dir (°)

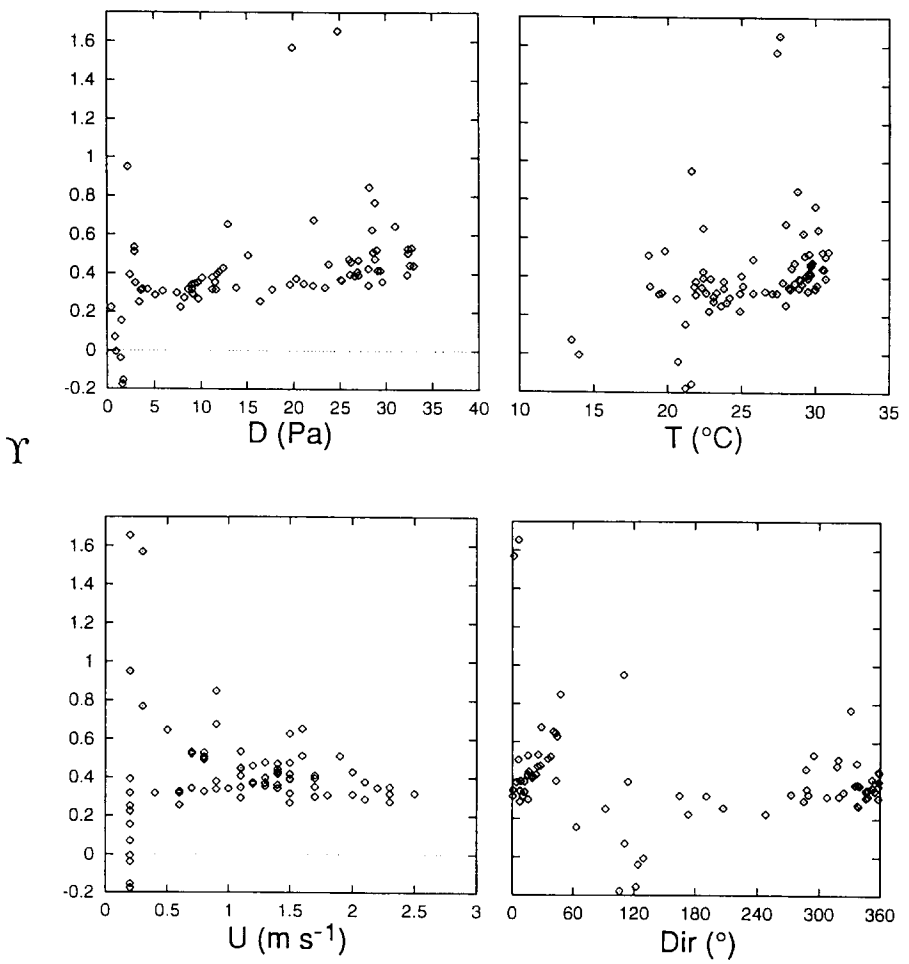

Fig. 5. (a) Relationship of latent heat flux to ambient meteorological variables: Q^*, net all-wave radiation (W m^{-2}); D, vapor pressure deficit (Pa); T, temperature (°C); U, wind speed (m s^{-1}); Dir, wind direction (degrees). (b) Relationship of Υ (Q_E/Q^*) to ambient meteorological variables.

temperature and available energy ($Q^*-\Delta Q_S$). Temperature is used to determine the slope of the saturation vapor pressure vs. temperature curve (s) and in the calculation of the psychrometric 'constant' (γ). The models differ in that the Penman model also considers the role of the vapor pressure deficit (D) and wind speed (U).

A common input requirement for both models is the storage heat flux. Given the broader objective of this study, to investigate the longer-term hydrological behavior of the wetland system for periods when the energy balance fluxes are not measured (i.e. when the storage term cannot be determined as a residual), a prerequisite is to develop a simple model of the storage heat flux, which can then be used as input to the evaporation model. The approach described here parameterizes the storage heat flux in terms of the net all-wave radiation which forces the energetics of the system. The use of this type of model in conjunction

with the evaporation models has the significant advantage of not requiring any additional data inputs.

4.1. Storage heat flux models

A common approach to estimate the storage term, when direct observations are not available, is to calculate it as a simple linear fraction of the net all-wave radiation (see, e.g. Idso et al. (1975)). However, in many environments (see, e.g. the work of Camuffo and Bernardi (1982) and Grimmond et al. (1991)), and as documented here, the diurnal pattern of the storage heat flux exhibits distinct hysteresis; values are higher in the morning and lower in the afternoon (Fig. 6). Recognizing this, Camuffo and Bernardi (1982) proposed the following form of equation to model the storage heat flux:

$$\Delta Q_S = a_1 Q^* + a_2 \frac{\partial Q^*}{\partial t} + a_3 \tag{4}$$

where t is time, and a_1, a_2 (h), and a_3 (W m^{-2}) are empirically determined coefficients. The parameter a_1 indicates the overall strength of the dependence of the storage heat flux term on net radiation. The parameter a_2 describes the degree and direction of the phase relationship between ΔQ_S and Q^*; when a_2 is positive, the net radiation lags behind the ΔQ_S curve on a diurnal basis; when it is zero, no hysteresis is present in the relationship and the two curves are exactly in phase. The parameter a_3 is an intercept term. In this study, $\partial Q^*/\partial t$ is

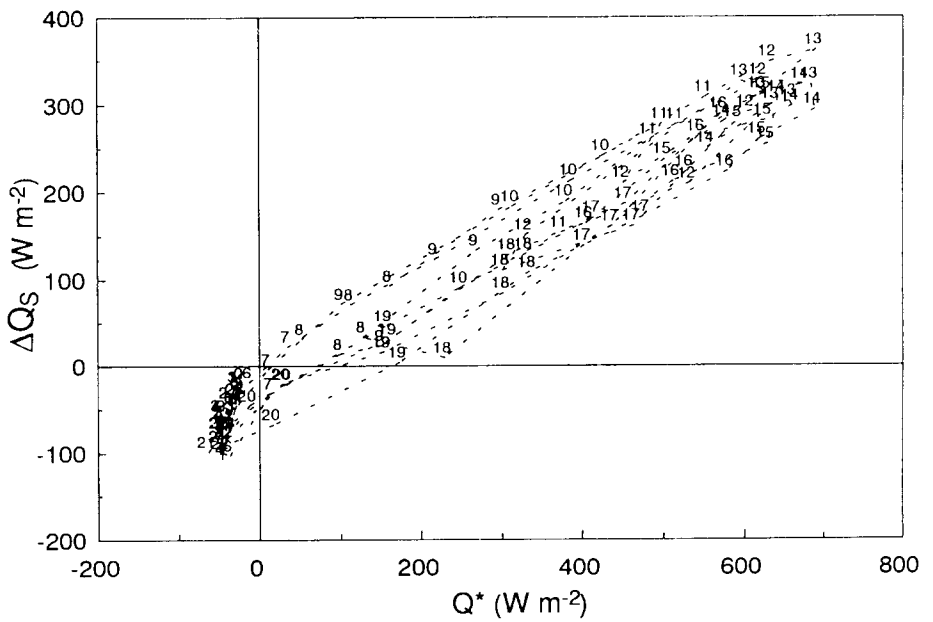

Fig. 6. Observed daily hysteresis of the storage heat flux. The numbers on the graph indicate the time at the end of the hour of observation. (Note some days are incomplete (see Fig. 3).)

calculated using hourly data:

$$\frac{\partial Q^*}{\partial t} = 0.5[Q^*_{t+1} - Q^*_{t-1}] \tag{5}$$

Thus the storage heat flux density is expressed both as a function of net all-wave radiation, and the rate and direction of change in radiant forcing.

For this study, three different forms of storage heat flux model were fitted to the available data: (1) a linear model; (2) a hysteresis model using all available data; (3) a hysteresis model with coefficients calculated separately for daytime ($Q^* > 0$) and nighttime ($Q^* < 0$) hours.

The fitted linear model (ΔQ_{S_L}) takes the form

$$\Delta Q_{S_L} = 0.537Q^* - 37.5 \tag{6}$$

The hysteresis model developed with all available data ($\Delta Q_{S_{H1}}$) has the coefficients

$$\Delta Q_{S_{H1}} = 0.537Q^* + 0.215\frac{\partial Q^*}{\partial t} - 30.4 \tag{7}$$

The hysteresis model developed separately for day and night, for daytime hours ($Q^* > 0$) is expressed as

$$\Delta Q_{S^d_{H2}} = 0.523Q^* + 0.215\frac{\partial Q^*}{\partial t} - 30.4 \tag{8}$$

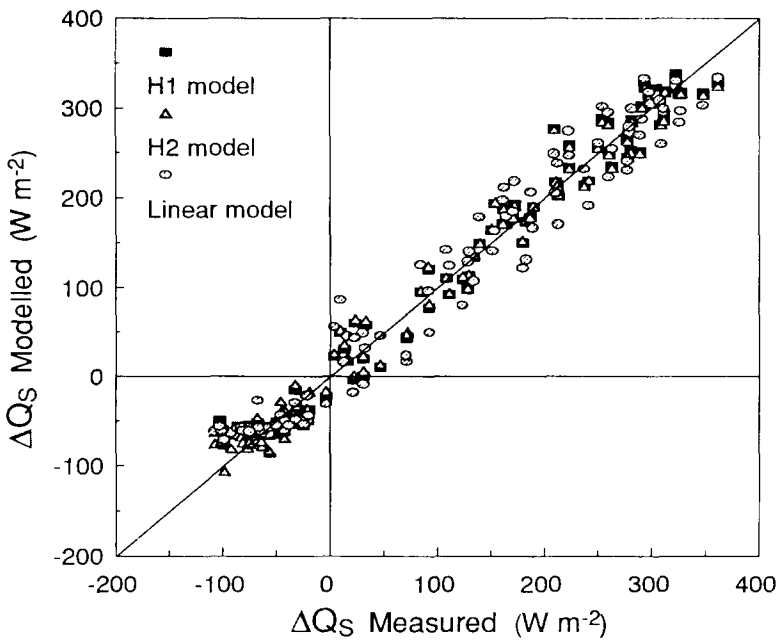

Fig. 7. Performance of the three storage heat flux models (see text for explanation).

Table 3
Statistics for hourly storage heat flux (ΔQ_S) (n = 100) and latent heat flux (Q_E) (n = 107) model evaluations (see text for model notation; flux units are W m^{-2})

	ΔQ_S			Q_E				
	ΔQ_{S_L}	$\Delta Q_{S_{H1}}$	$\Delta Q_{S_{H2}}$	PTα = 1.26	Equil.α = 1.00	P1	P2	P3
Mean: $\overline{x_m}$	95.5	95.5	95.5	143.3	113.7	113.7	116.3	114.4
SD: SD_m	143.1	144.2	144.5	116.4	92.4	92.3	93.9	92.9
Slope	0.96	0.98	0.98	1.26	1	0.997	1.015	1.003
Intercept	3.7	2.2	1.9	1.9	1.5	1.5	2.0	1.5
r^2	0.961	0.977	0.980	0.954	0.954	0.954	0.957	0.955
r.m.s.e.	28.8	22.2	20.6	45.8	19.8	19.8	19.9	19.8
r.m.s.e.—sy	5.7	3.4	2.9	38.5	1.2	1.2	4.0	1.9
r.m.s.e.—usy	28.2	22.2	20.4	24.9	19.7	19.7	19.5	19.7
d	0.990	0.994	0.995	0.952	0.988	0.988	0.988	0.988
n&s	0.961	0.977	0.980	0.743	0.952	0.952	0.952	0.952
MBE	0.0	−0.0	−0.0	30.8	1.2	1.2	3.8	1.8
MAE	23.2	18.4	16.5	35.8	15.7	15.7	15.9	15.8

Mean observed storage heat flux (ΔQ_S) 95.5 W m^{-2}, standard deviation (SD) 145.9 W m^{-2}; mean observed latent heat flux (Q_E) 112.6 W m^{-2}, SD 90.5 W m^{-2}. The slope, intercept and r^2 (correlation coefficient) refer to the linear fit between the observed (o) and the modelled (m) data. The root mean square error (r.m.s.e.) consists of systematic (sy) and unsystematic (usy) portions (W m^{-2}). d, Index of agreement (Willmott, 1981); n&s, goodness of fit (Nash and Sutcliffe, 1970); MBE, mean bias error; MAE, mean absolute error.

and for night-time ($Q^* < 0$) hours as

$$\Delta Q_{S_{H2}}^{n} = 1.657Q^* + 0.094\frac{\partial Q^*}{\partial t} + 1.1 \tag{9}$$

Fig. 7 illustrates the performance of the fitted models. The $\Delta Q_{S_{H2}}$ model has the best performance (Table 3), with the lowest overall systematic and unsystematic root mean square errors (r.m.s.e.). The hysteresis models remove the scatter that is present with the linear model. By stratifying the data and calculating model coefficients separately for day and night, the fit for the night-time hours is improved (see Fig. 7). Obviously, there is a need to verify all of these results with an independent data set. The ΔQ_S values used in the subsequent analyses are those modeled using the $\Delta Q_{S_{H2}}$ model.

4.2. Latent heat flux models

The Priestley and Taylor (1972) evaporation model is a commonly used operational procedure to estimate evaporation from wetlands (for examples of its application, see Roulet and Woo (1986), Price and Woo (1988) and Price (1992)):

$$Q_{E_{PT}} = \alpha_{PT}\frac{s}{s+\gamma}(Q^* - \Delta Q_S) \tag{10}$$

The psychrometric 'constant', γ, is determined from

$$\gamma = \frac{c_p P}{\epsilon L_v} \tag{11}$$

where c_p is the specific heat of moist air (1010 J kg^{-1} K^{-1}), P is atmospheric pressure, ϵ is the ratio of molecular weight of water vapor to that for dry air (0.622), and L_v is the latent heat of vaporization, which in this study was calculated using the method of Henderson Sellers (1984). The equations of Lowe (1977) are used to determine s. When $\alpha = 1$, this equation becomes the equilibrium evaporation model, which describes evaporation when there is no vapor pressure deficit in the atmosphere. In practice (on average) some vapor deficit always exists. Priestley and Taylor (1972) found that over ocean and saturated land α_{PT}, the empirical coefficient, equals 1.26. This figure has become the normally quoted average value for potential evapotranspiration from a wet surface or small lake (see, e.g. Stewart and Rouse (1976) and de Bruin and Keijman (1979)). However, many experimental values for well-watered surfaces show a departure of α_{PT} from 1.26 (Monteith, 1981). Ingram (1983) concluded that the relationship between actual and potential evaporation for wetlands depends largely on the vegetation; ratios for treeless bogs lie between 1.0 and 1.1, whereas for fens the quotient is about 1.4 or a little less.

Measured hourly evaporation from the wetland was compared with two forms of the Priestley–Taylor model: the first with $\alpha = 1.26$, the second substituting $\alpha = 1.00$ (Fig. 8, Table 3). In addition, α was back-calculated from the measured data by substituting actual evaporation and solving for α. Eq. (10) can be rearranged to

$$\alpha = \left[\frac{s}{s+\gamma}(1+\beta)\right]^{-1} \tag{12}$$

This form has the advantage that data only directly measured in this study are used to determine α, including β, the ratio of the two directly measured fluxes (Q_H/Q_E). Based on the ensemble hourly results the mean back-calculated α was determined as 1.035.

Penman (1948), using a combination of the energy balance and bulk transfer formulae, derived an equation for evaporation from open water and saturated land surfaces. Penman's formula, either in the original or slightly modified form, is widely used for estimating potential evaporation (for examples of its application in wetland environments, see Koerselman and Beltman (1988) and Lafleur (1990b)).

The original Penman model implicitly assumed a roughness length, and, as expressed by Shuttleworth (1992), has the form

$$Q_{E_{PI}} = \frac{s}{s+\gamma}(Q^* - \Delta Q_S) + \frac{\gamma}{s+\gamma}[6.43(1+0.536U)D] \tag{13}$$

The Penman model was modified by Monteith (1965) to incorporate aerodynamic and surface resistance controls. The Penman–Monteith model is the most advanced resistance-based model of evaporation that is currently commonly used (Shuttleworth, 1992):

$$Q_{E_{PM}} = \frac{s(Q^* - \Delta Q_S) + \rho_a c_p D/r_a}{s+\gamma(1+r_s/r_a)} \tag{14}$$

where ρ_a is the density of air, D is the vapor pressure deficit, r_a is the aerodynamic resistance, and r_s is the surface resistance. Under potential evaporation conditions the surface resistance (r_s) equals zero.

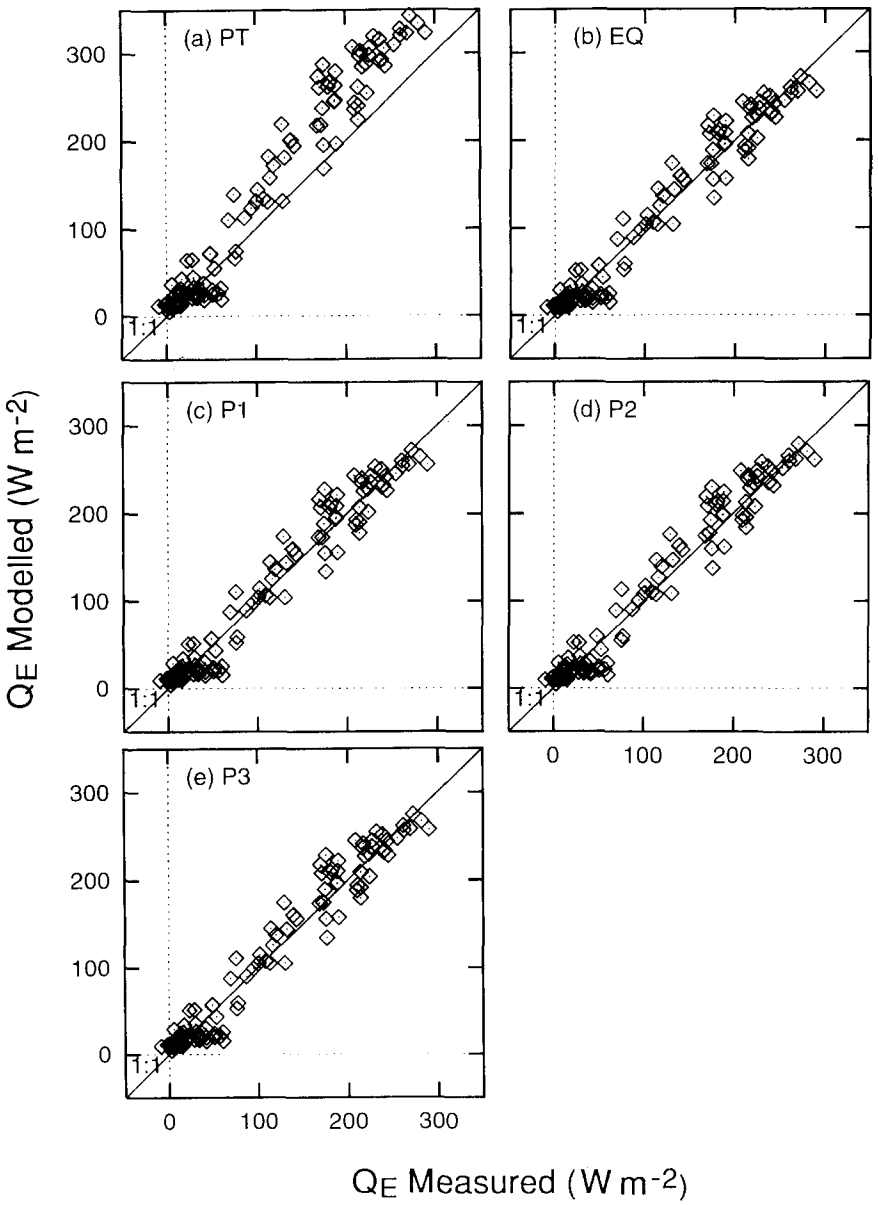

Fig. 8. Performance of latent heat flux models (see text for explanation): (a) Priestley–Taylor (PT); (b) equilibrium (EQ); (c) Penman 1 (P1); (d) Penman–Monteith 2 (P2); (e) Penman–Monteith 3 (P3).

Aerodynamic resistance (r_a) can be determined either by the method of Thom and Oliver (1977):

$$r_a = \frac{4.72\{\ln[(z_m - d)/z_0]\}^2}{1 + 0.536U} \tag{15}$$

where z_m is the observation height, d is the displacement length, and z_0 is the roughness length, or using the method of Thom (1972):

$$r_a = \frac{\{\ln[(z_m - d)/z_0] - \psi\}\{\ln[(z_m - d)/z_{0v}] - \psi_v\}}{k^2 U} \quad (16)$$

where ψ and ψ_v are stability functions for momentum and water vapor, respectively, z_{0v} is the water vapor roughness length, and k is the von Kármán constant (0.4).

In this study, the original Penman equation (Eq. (13); P1), the Penman–Monteith model using Eq. (15) to calculate r_a (P2), and the Penman–Monteith model using Eq. (16) to calculate r_a (P3), were evaluated. The stability conditions are assumed to be neutral, which Shuttleworth (1989) found to be satisfactory over forests. The roughness length and displacement length were determined as a function of the height of the vegetation (z_v, maximum height of vegetation 1.5 m, average height approximately 1.0 m) following 'rules of thumb' ($z_0 = 0.11z_v$; $d = 0.667z_v$) (Stull, 1988). Following Brutsaert (1982) z_{0v} was taken to be $0.1z_0$. Vapor pressure deficit (D) was determined from observations of air temperature and relative humidity, and the Lowe (1977) equation for saturation vapor pressure (e_s).

The results of the latent heat flux model comparisons are shown statistically in Table 3 and graphically in Fig. 8. There is very little difference between the equilibrium Q_E (i.e. Eq. (10) with $\alpha = 1$) and the original Penman equation (Eq. (13)), both of which perform well. The energy term (left-hand side of Eq. (13)) is by the far the most significant control on Q_E (discussed above and indicated in Fig. 4). As noted above, the Great Marsh is located in close proximity to a large water body in a humid temperate environment, and is significantly affected by the local-scale daytime flow of humid air. Practically at this site the aerodynamic term (right-hand side of Eq. (13)) does not warrant inclusion, given the extra data requirements. The P2 and P3 forms of the Penman model, which require further specification of the surface, through z_0 and d, also do not provide any improvement in model performance. The results also suggest that the assumption of neutral stability (i.e. neglect of the stability functions in Eq. (16)) is reasonable in this context, and any resulting errors are small. It is likely that the mis-specification of the surface parameters is more likely to introduce greater error than improve model performance. The Priestley–Taylor α_{PT} of 1.26 is clearly not appropriate for this wetland system (see Table 3, most notably the slope between measured and observed data).

5. Conclusions

The eddy correlation determination of the turbulent fluxes reported in this study are among the first for wetlands. Overall, latent heat flux dissipated 48% of the available radiant energy, storage heat flux 35%, and sensible heat flux 17%. In the morning, when the atmosphere is fairly stable and wind speeds are low, the air above the wetland is virtually saturated. Thus the radiant energy is used to warm the Great Marsh. Later in the day, as the atmosphere becomes more unstable and the wind picks up, the turbulent transfer of heat into the atmosphere is enhanced and the latent and sensible heat fluxes become more significant. The latent heat flux is strongly related to net all-wave radiation,

and is suppressed by the flow of humid air off Lake Michigan (very similar to the equilibrium rate, average $\alpha = 1.035$).

The hysteresis storage heat flux model presented here works well and offers great potential. It has the advantage of only requiring data on net all-wave radiation; consequently, the storage heat flux, essential for latent heat flux modeling, can be estimated relatively easily. The relative success of the simple models (Penman and Priestley–Taylor $\alpha = 1$), with their very limited data requirements, indicates they are appropriate for longer-term modeling of energy and water exchanges in this type of wetland environment. Although the modeling here is conducted at an hourly time scale, model performance is generally better when time periods are aggregated. There is an obvious need to collect more flux data to independently assess both the temporal and spatial performance of the models, as well as the numerical stability of the empirical coefficients. In addition, direct observations of the storage heat flux term need to be conducted at the same time as the eddy correlation flux data collection.

Acknowledgements

Assistance in the field by Mark McKee, Tom King, and Mark Hubble was greatly appreciated. This research was supported by Indiana University Purdue University Indianapolis, Indiana University Bloomington, Save the Dunes Council, National Biological Service, Indiana Dunes State Park and Nature Preserve, and Indiana Dunes National Lakeshore.

References

Brutsaert, W., 1982. Evaporation into the Atmosphere. D. Reidel, Dordrecht, 299 pp.

Camuffo, D. and Bernardi, A., 1982. An observational study of heat fluxes and the relationship with net radiation. Boundary-Layer Meteorol., 23: 359–368.

de Bruin, H.A.R. and Keijman, J.Q., 1979. The Priestley–Taylor evaporation model applied to a large shallow lake in the Netherlands. J. Appl. Meteorol., 18: 898–903.

Grimmond, C.S.B., Cleugh, H.A. and Oke, T.R., 1991. An objective urban heat storage model and its comparison with other schemes. Atmos. Environ., 25B: 311–326.

Halliwell, D.H. and Rouse, W.R., 1987. Soil heat flux in permafrost: characteristics and accuracy of measurement. J. Climatol., 7: 571–584.

Henderson Sellers, B., 1984. A new formula for latent heat of vaporization of water as a function of temperature. Q. J. R. Meteorol. Soc., 110: 1186–1190.

Idso, S.B., Aase, J.K. and Jackson, R.D., 1975. Net radiation–soil heat flux relations as influenced by soil water content variations. Boundary-Layer Meteorol., 9: 113–122.

Ingram, H.A.P., 1983. Hydrology. In: A.J.P. Gore (Editor), Mires: Swamp, Bog, Fen and Moor. Elsevier, New York, pp. 67–158.

Koerselman, W. and Beltman, B., 1988. Evapotranspiration from fens in relation to Penman's potential free water evaporation and pan evaporation. Aquat. Bot., 31: 307–320.

Lafleur, P.M., 1990a. Evaporation from wetlands. Can. Geogr., 34: 79–88.

Lafleur, P.M., 1990b. Evaporation from sedge-dominated wetland surfaces. Aquat. Bot., 37: 341–353.

Latimer, J.R., 1972. Radiation measurement. Int. Field Year for the Great Lakes Tech. Manual Ser. 2. NRC–USNAS–IHD, Ottawa, Ont., 53 pp.

Linacre, E.T., 1976. Swamps. In: J.L. Monteith (Editor), Vegetation and the Atmosphere, Vol. 2. Case Studies. Academic Press, Bristol, pp. 329–350.

Linacre, E.T., Hicks, B.B., Sainty, G.R. and Grauze, G., 1970. The evaporation from a swamp. Agric. Meteorol., 7: 363–374.

Loiacono, N.J., 1986. Hydrologic and hydrochemical characterization of the shallow ground-water system of the Great Marsh, Indiana Dunes National Lakeshore. M.Sc. Thesis, Purdue University, West Lafayette, IN, 118 pp.

Lowe, P.R., 1977. An approximating polynomial for the computation of saturation vapor pressure. J. Appl. Meteorol., 16: 100–103.

Monteith, J.L., 1965. Evaporation and the environment. Symp. Soc. Exp. Biol., 19: 205–234.

Monteith, J.L., 1981. Evaporation and surface temperature. Q. J. R. Meteorol. Soc., 167: 1–27.

Nash, J.E. and Sutcliffe, J.V., 1970. River flow forecasting through conceptual models. Part I—a discussion of principles. J. Hydrol., 10: 282–290.

NOAA, 1994. South Bend Local Climatological Data. National Oceanic and Atmospheric Administration, US Department of Commerce, Asheville, NC.

Oke, T.R., 1987. Boundary Layer Climates, 2nd edn. Methuen, London, 435 pp.

Penman, H.L., 1948. Natural evaporation from open water, bare soil and grass. Proc. R. Soc. London, Ser. A, 193: 120–145.

Price, J.S., 1992. Blanket bog in Newfoundland. Part 2. Hydrological processes. J. Hydrol., 135: 87–101.

Price, J.S. and Woo, M.K., 1988. Studies of a subarctic coastal marsh. I. Hydrology. J. Hydrol., 103: 275–292.

Priestley, C.H.B. and Taylor, R.J., 1972. On the assessment of surface heat flux and evaporation using large scale parameters. Mon. Weather Rev., 100: 81–92.

Roth, M. and Oke, T.R., 1994. Comparison of modelled and measured heat storage in suburban terrain. Beitr. Phys. Atmos., 67: 149–156.

Roulet, N.T. and Woo, M.K., 1986. Wetland and lake evaporation in the low Arctic. Arct. Alp. Res., 18: 195–200.

Rouse, W.R., Hardill, S.G. and Lafleur, P., 1987. The energy balance in the coastal environment of James Bay and Hudson Bay during the growing season. J. Climatol., 7: 165–179.

Shedlock, R.J., Cohen, D.A., Imbrigiotta, T.E. and Thompson, T.A., 1994. Hydrogeology and hydrochemistry of dunes and wetlands along the southern shore of Lake Michigan, Indiana. US Geol. Surv. Open-File Rep., 92-139: 85 pp.

Shuttleworth, W.J., 1989. Micrometeorology of temperate and tropical forests. Philos. Trans. R. Soc. London, Ser. B, 324: 199–224.

Shuttleworth, W.J., 1992. Evaporation. In: D.R. Maidment (Editor), Handbook of Hydrology. McGraw–Hill, New York, pp. 4.1–4.53.

Silis, A., Rouse, W.R. and Hardill, S., 1989. Energy balance of the intertidal zone of western Hudson Bay: I. Ice-free period. Atmos. Ocean, 27: 327–354.

Stewart, R.B. and Rouse, W.R., 1976. Simple models for calculating evaporation from dry and wet surfaces. Arct. Alp. Res., 8: 263–274.

Stull, R.B., 1988. An Introduction to Boundary Layer Meteorology. Kluwer Academic, Dordrecht, 666 pp.

Tanner, B.D. and Greene, J.P., 1989. Measurements of sensible heat flux and water vapor fluxes using eddy correlation methods. Final report to US Army Dugway Proving Grounds, DAAD 09-87 D-0088, 94 pp.

Thom, A.S., 1972 Momentum, mass and heat exchange of vegetation. Q. J. R. Meteorol. Soc., 99: 154–170.

Thom, A.S. and Oliver, H.T., 1977. On Penman's equation for estimating regional evaporation. Q. J. R. Meteorol. Soc., 193: 345–357.

Thompson, T.A., 1987. Sedimentology, internal architecture and depositional history of the Indiana Dunes National Lakeshore and State Park. Ph.D. Thesis, Indiana University, Bloomington, IN, 129 pp.

Webb, E.K., Pearman, G.I. and Leuning, R., 1980. Correction of flux measurements for density effects due to heat and water vapour transfer. Q. J. R. Meteorol. Soc., 106: 85–100.

Wessel, D.A. and Rouse, W.R., 1993. Modelling evaporation from wetland tundra. Boundary-Layer Meteorol., 68: 109–130.

Wilhelm, G.S., 1990. Report on the special vegetation of the Indiana Dunes National Lakeshore. Indiana Dunes National Lakeshore Research Program, Rep. 90-2, 373 pp.

Willmott, C.J., 1981. On the validation of models. Phys. Geogr., 2: 184–194.

Winter, T.C., 1981. Uncertainties in estimating the water balance of lakes. Water Resour. Bull., 17: 82–115.

WMO, 1966. Measurement and estimation of evaporation and evapotranspiration. World Meteorological Organization, Geneva, Technical Note 83.